ISSN: 2476- 2334

Research Article

International Journal of Nanotechnology and Nanomedicine

Development of Nanostructured-based Composites as Advanced Thermal Interface Materials

Vignesh Varadaraju and Pradip Majumdar*

Department of Mechanical Engineering, Northern Illinois University, DeKalb, Illinois 60115, USA

***Corresponding author**
Pradip Majumdar, Department of Mechanical Engineering, Northern Illinois University, DeKalb, Illinois 60115, USA

Submitted: 31 Dec 2019; **Accepted**: 08 Jan 2020; **Published**: 29 Feb 2020

Abstract

Thermal management is one of the most critical issues in electronics due to increasing power densities. This problem is getting even worse for small and sophisticated devices due to air gaps present between the heat source and heat sink. Thermal interface materials (TIM) are used to reduce the air gaps and significantly increase the heat transfer capability of the system. A high-thermal-performance, cost-effective and reliable TIM would be needed to dissipate the generated heat, which could enable significant reductions in weight, volume and cost of the thermal management system. In this study a number of different nanostructured materials are reviewed for potential use as a filler material in our effort to develop advanced TIM composite. Some of the candidate filler materials considered is Carbon Nanotubes, Graphene and Few Layer Graphene (FLG), Boron Nitride Nanotubes (BNNT) and Boron Nitride Nanomesh (BNNM) and Boron Arsenide (BAs). Objective is to identify composition of boron arsenide as filler in polymer-nanostructured material composite TIM for high heat flux applications. In order to design boron-arsenide-based TIM composite with enhanced effective thermal conductivity, a number of metallic and nonmetallic base-filler material composites are considered with varying filler fractions. Empirical mixture models based on effective medium theories (EMT) are evaluated for estimating effective conductivity of the two-component boron arsenide-filler composite TIM structure.

Introduction

The invention of high-speed electronics devices has been consistently increasing along with the need for an efficient thermal management system to meet the demand for dissipating the high heat flux losses and reduce the junction temperature to sustain operation.Air gaps that exist between the heat source and heat sink increase the resistance to heat flow between them. Excessive heat accumulated in electronics system reduces performance and causes wear and premature failure of the system. Space power electronics components have specifically called for the objective as to reduce the thermal resistance between silicon carbide-based power module components and cold plates by a sizable factor. In addition to the needed high conductivity, the space applications require vacuum-compatible interface materials in order to reduce interface temperature gradients to facilitate efficient heat removal.

Thermal interface material (TIM) is used to fill the air gaps to reduce the resistance between the heat source and heat sink. The use of TIM in electronics devices, subject to localized high heat flux at the interface of dissimilar material, reduces the net thermal resistance from the conduction heat dissipation path from heat-generating modules to the heat source to the heat sink. Apart from electronics devices, TIM is widely used in medical instruments, data centers, aerospace applications, LED appliances and other heat-generating devices. Improper selection of TIM in terms of bond line thickness (BLT), melting point, reliability, material properties, etc., increases the interfacial thermal resistance and contact resistance. Conventional TIMs such as wax, grease, thermal tapes, gels and pads face challenges to satisfy the above-mentioned requirements due to decrease in size and increased speed, reliability of the new generation of electronics and power modules systems.

Developing an efficient TIM in terms of cost and reliability would suffice for existing problems associated with the thermal management system. The characteristics of an efficient TIM are high thermal conductivity, low interfacial thermal resistance, low contact resistance, low BLT, etc. Fractional change in the resistance value and thermal conductivity of TIM has greater influence on the heat transfer rate between the heat source and heat sink. There is rapidly increasing demand for thermally efficient power electronics systems and therefore increasing demand for the development of advanced thermal interface (TIM) materials. There has been interest in maturation of nanostructure-based materials like nanotubes, graphene, diamond, boron arsenide technology and material systems. In that line, the intent is to develop more reliable thermal interface materials that are not only exhibit few order of magnitude enhancement in effective thermal conductivity specially to meet the cross-plane effective thermal conductivity enhancement of the order of 500% by meeting the goals of 20 to 25 W/m-K.Recently it has been identified in the literature that boron arsenide has a diamond-like thermal conducting material, but it has challenges in its synthesis and quality for tailoring reliable performance.It is believed

that advanced next-generation thermal management materials that maintain a significantly reduced interfacial thermal resistance throughout the life of the system plays a major role in making key improvements in the efficiency of the thermal management sub systems.

Lindsay, et al. has calculated the thermal conductivities of cubic III-V boron compounds using a predictive first principles approach [1]. Boron arsenide is found to have a remarkable thermal conductivity of over 2000 W/m.K due to fundamental vibration properties, some of which are not typically connected to prescriptions for high thermal conductivity in materials. The large arsenic to boron mass ratio and the unusual, almost purely covalent bonding in BAs give a large frequency gap between its acoustic and optic phonons (a-o gap) and bunching of the acoustic phonon dispersions; the intrinsic thermal conductivity is sensitive to the combination of these properties. Prasher, et al. has focused on bond linethickness (BLT) that can be obtained by rheological measurements from particle laden polymers (TIM) [2]. The silicone oil used is polydimethylsiloxane fluid of three viscosities. The interface resistance is higher for the surface with higher volume fraction due to imperfect wetting or mixing of the filler particles with the silicon oil, as the thermal conductivity of silicon oil is very low. After certain optimal loading and particle volume fraction ($\alpha<4$), if there is an increase in their ranges, the thermal resistance increases despite thermal conductivity.

Moore and Shi have discussed about the anisotropic thermal conductivities stating that the basal-plane thermal conductivity of 2D layered materials can be exceptionally high, and the cross-plane value can be more than an order of magnitude lower [3]. They have examined a few cubic crystals, two-dimensional layered materials, nanostructure networks and composites, molecular layers and surface functionalization, and aligned polymer structures for potential applications as heat spreading layers and substrates, thermal interface materials, and underfill materials in future-generation electronics. Jain and McGaughe have studied the competing effects of mass density, a-o gap, acoustic width, optical width, and acoustic bunching on the thermal conductivity of compound semiconductors, where the species differ only in mass [4]. They found that the thermal conductivity depends on the mass difference of the two species and how it affects the a-o gap and the acoustic-width. The thermal conductivity increases with increasing a-o gap to acousticwidth ratio, attains a maximum close to ratio of 1, and decreases with further increase in the ratio.

Pietrak and Wisniewski have reviewed the most popular expressions for predicting the effective thermal conductivity of composite materials using the properties and volume fractions of constituent phases [5]. Among effective medium theories (EMT), Bruggeman-type approximations, deal better with higher filler volume fractions than Maxwell-Eucken-type approximationsbut the latter are used more often due to their simplicity. For spherical particles, one of the most prominent models used is the Maxwell model which matches the experimental data for filler fraction up to 30 %. Wang and Mujumdar have reviewed about the research on theoretical and numerical investigations of various thermal properties and applications of nanofluids [6]. They have explained about several semi-empirical correlations used for calculating the apparent conductivity of two-phase mixtures and comparedthe selected theoretical models with experimental data for thermal conductivity of Al_2O_3/water nanofluids.

Kargar et al. have reported the results of an experimental study that compares the performance of graphene and boron nitride flakes as fillers in the thermal interface materials [7]. They have varied the thickness of both fillers from a single atomic plane to about a hundred atomic planes and the measurement of thermal conductivity has been conducted using a standard TIM tester. Sarvar, et al. have reviewed the state-of-the-art of thermal interface materials ranging from the conventional interface materials to advanced carbon nanotube-based materials; they discussed about the properties, advantages and disadvantages of each TIM category and the factors that need to be considered while selecting the thermal interface material [8]. They have also emphasized about the types of resistance and their effects associated with the thermal conductivity of thermal interface materials. Tao, et al. has proposed a percolation model to determine the effective thermal conductivity of the composite materials along with the methods to determine the percolation threshold and the exponent in the percolation model [9]. Percolation exponent is dependent on the filler size, filler shape, and filler distribution in the composites. Compared to other models proposed, theoretical results obtained with the percolation model agree better with the experimental data.

Syamala has developed a computational fluid dynamics (CFD) simulation to evaluate the graphene-based composites as thermal interface materials in aninsulated gate bipolar transistor (IGBT) package for high heat flux applications [10]. He found that the thermal interface materials based on FLG-metal composites showed superior thermal performance as compared to state-of-the-art TIMs such as thermal grease and Dow Corning TC5022.

In this study number of different nanostructured materials is reviewed for our potential use as a filler material in our effort to develop advanced TIM composite. Some of the candidate filler materials considered is Carbon Nanotubes, Graphene and Few Layer Graphene (FLG), Boron Nitride Nanotubes (BNNT) and Boron Nitride Nanomesh (BNNM) and Boron Arsenide (BAs) our effort is further concentrated on development of advanced thermal interface materials TIMs based on the use of nanostructured materials like boron-arsenide-based composites. Objective is to identify composition of boron arsenide as filler in polymer-nanostructured material composite TIM for high heat flux applications. In order to design boron-arsenide-based TIM composite with enhanced effective thermal conductivity, a number of metallic and nonmetallic base-filler material composites are considered with varying filler fractions. Empirical mixture models based on effective medium theories (EMT) are evaluated for estimating effective conductivity of the two-component boron arsenide-filler composite TIM structure.

Nanostructured-based Composites

In this section, a few advanced thermal interface materials are discussed in contrast with the common TIMs. Common TIMs are the composite mixture of thermally conducting metallic or ceramic fillers that are space qualified and vacuum compatible polymeric materials. Major requirements are high thermal conductivity and compliance. Such common TIMs require large volume fractions fillers. Polymeric composites with a high thermal are always desired for wide variety of applications. While improved thermal conductivity of polymers can be achieved through dispersion of metallic particles in a polymer matrix, a good dispersion and thermal coupling is quite a challenge. Thermal resistance and reliability of the interface material must be improved significantly for effective use in high temperature and

high heat flux electrical power systems.

In recent years, major research effort on the development of high thermal conductivity thermal interface materials are concentrated around the use of high thermal conductivity materials like carbon nanotubes – SWNTs and MWNTs, aluminum nitride (AIN), bi-layer graphene and few layer graphene, and boron nitride nanotubes – high-K BNNTs.Carbon nanotubes (CNTs- SWNTs), boron nanotubes (BNTs and graphene –bilayer and few layer graphene (FLG) are some of the novel materials that have been considered for the development of new generation TIMs with reduced thermal resistance.

Carbon Nanotube-Composites

Carbon nanotubes (CNTs) have been extensively considered as a novel TIM material due to its very high thermal conductivity values. However, CNT films involve high interface resistance due to poor contacts of the NTs with the substance surfaces; an effect referred to as the Kapitza resistance, and failed to provide the anticipated performance. Some of the CNT-TIM sample analyzed aremetal-CNT composites; CNT-Cunanocomposites; CNT-copper nanocomposite; CNT-Al and CNT -Al alloy composites. For 10 micron thick metal-SWNT and SWNT-substance interfaces, thermal interface resistances value of 3.8 mm^2.K/W and 9.2 mm2.K/W respectively are reported. Reported values for vertically oriented CNT interface resistances in Si-CNT-Ag and Si-CNT-CNT-Cu contact surface are of the order of 15.8 mm^2.K/W, and silicon-CNT-silver has a thermal interface resistance in the range of 7 – 19 mm2.K/W.

Few Layer Graphene (FLG) and Graphene Composites

Graphene is two-dimensional a monolayer graphite with over 100-order anisotropy of heat flow between the in-plane and cross-plane directions. Graphene possesses one of the highest in-plane thermal conductivity of the order of 2000-4000 W/m.K for suspended graphene. In comparison thermal conductivity of natural diamond is 2200 W/m.K at room temperature [11]. The high in-plane thermal conductivity is due to covalent bonding between carbon atoms and the out-of-plane conductivity is due to the weak van-der-waals coupling force. The in-plane thermal conductivity of graphene, however, decreases considerably when supported with a substrate or encased/confined due to weak thermal coupling caused by van der Waals interactions and interaction/scattering of graphene phonon with the substrate phonons. Thermal conductivity of graphene supported by silicon substrate is reported as 600 W/m.K.

Thermal properties like specific heat and thermal conductivity of nano- or micro-structured materials are linked to the phonon transport phenomena involving multiple acoustic and optical vibration modes of lattice structure. A graphene unit lattice cell structure is subjected to three acoustic modes and three optical phonon modes. The Theoretical modeling of thermal conductivity requires consideration of solid-state physics and consideration dispersion curves, a relationship between the phonon energy, E or frequency, ω and phonon wave or group velocity.

Thermal conductivity graphene also decreases as it stacks into layers like in few layer graphene (FLG) which are then subjected to cross-plane heat dissipation with van-der-waals interaction and phonon scattering in between layers [12]. Singh, et al. have demonstrated their theoretical analysis based on phonon-phonon interactions and linearized Boltzmann transport equation that out-of-plane thermal conductivity dropped sharply from a single-layer graphene to two-layer grapheme [13]. With further increase of layers to three or four, the decrease is less with increase in layers and remains unchanged by four layers. At about 300K, the thermal conductivity (about 3000 W/m.k) dropped by 29% for two layers to 37% to 35% and 37% (2000 W/m.K) for three layers and four layers respectively.

Few layer graphene (FLG) and graphene composites are also considered increasing as a viable improved low thermal resistance interface material. Few layer graphene (FLG) Composite of optimized mixture graphene as the fillers and a range of matrix materials such as metallic micro – and nanoparticles are considered at NIU. Results for enhanced thermal conductivity by a factor of ~ 23 is achieved with commercially available TIM mixed with 10 % loading of graphene as thermally conductive filler.

MWNT- graphene nanoplatelet composite (20 % MWNT-80% graphene nanoplatelets) was also considered. Graphene nanoplatelets are the early versions of the graphite graphene with 10 to 20 layers. One of the major huddles in development and commercialization of graphene-based nanocomposites is the difficulty associated with the synthesis and large volume production of high quality FLGs with thickness restricted to 3-4 layers only. Additionally, the expense of graphene production is very high due to the restriction on the base starting material-graphite, which is limited in resources.

Boron Nitride Nanotubes (BNNT) and Boron Nitride Nanomesh (BNNM)

Boron nitride nanotubes (BNNTs) also exhibit very high thermal conductivities. However, large-scale production of BNNTs remains a major challenge for commercialization. The most commonly use methods for preparation of BNNTs include ball milling and annealing, arc discharge, chemical vapor deposition, laser ablation, mechano-thermal and other chemical syntheses techniques. Many of them use drastic reaction condition, e.g., high reaction temperature (in the range of 1273-1673 K) and needed expensive and complicated reaction setups. Therefore, a simple way of manufacturing large scale BNNTs is warranted.

BNNT and BNNM-based composites are also considered at NIU. NIU-AMSENG collaborative research included synthesis and processing of hexagonal-BN (h-BN) and development of BNNT-based TIMs. A successful method has been developed to prepare h-BN in relatively lower temperature and high yield. The fabrication process involves pyrolysis of boron and nitrogen containing precursors in the presence of certain catalysts in a sealed autoclave.

Boron Arsenide (BAs)

Boron arsenide is a chemical compound of boron and arsenic with a remarkable thermal conductivity of over 2000 W/m-K at room temperature; this is comparable to those in diamond and graphite. The large arsenic to boron mass ratio and the pure covalent bonding in BAs give a large frequency gap between its acoustic and optic phonons (a-o gap) and give a bunching of the acoustic phonon dispersions.

In semiconductors, heat is carried by vibrational waves of the constituent atoms, and the collision of these waves with each other creates an intrinsic resistance to heat flow, but this unusual interplay of certain vibrational properties in boron arsenide that lie outside of the guidelines are commonly used to estimate the thermal conductivity.BAs is unusual in that the acoustic branch

bunching weakens as scattering, the a-o gap is large enough to freeze out all associated processes, and its stiff bonding and small MB give a relatively large Debye temperature. This combination of features is not present in the other materials, and hence gives BAs anomalously large intrinsic phonon transport lifetimes and correspondingly ultra-high thermal conductivity from the mid-high frequency acoustic phonons.

Isotopic scattering can play an important role in determining the thermal conductivity in many material systems, such as those considered here. BAs have a large mixture of B isotopes; however, it has relatively small contributions from isotopic scattering, smaller even than cubic BN, and diamond. The reason for this is that for BAs, the large As to B mass ratio causes the atomic motion of the short wavelength acoustic phonons, which give the largest contributions to thermal conductivity, to be dominated by the heavier As mass, and As happens to be isotopically pure [1]. Figure 1 shows the characteristics of optic phonons and acoustic phonons that predicted the high thermal conductivity of boron arsenide.

In an effort to identify new high thermal conductivity of non-metallic crystal structure materials. Lindsay, et al. identified boron arsenide as one of the most promising materials considering the general rule that thermal conductivity decreases with increasing atomic mass and with decreasing Debye temperature [1]. With these general rules, they considered due to the following key factors: simple crystal structure, low average atomic mass, and strong interactive bonding, which implies a large Debye temperature. A first principle analysis was carried out based on the phonon dispersion curve data and solution of linearized Boltzmann transport equation for phonons for a class of boron-based cubic III-V compounds.

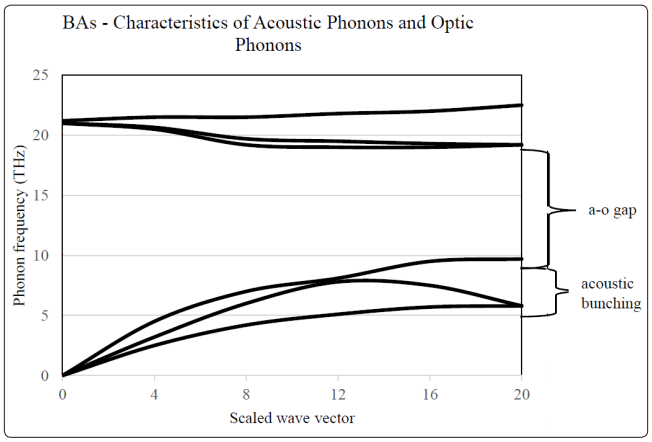

Figure 1: BAs – Characteristics of Acoustic Phonons and Optic Phonons

Figure 2 shows the variation of thermal conductivity with respect to temperature for diamond, graphene, boron arsenide and boron nitride. Among all boron compounds, and thermal conductivity of BAs is found to be considerably higher than those for all other materials. At room temperature, the value is about 2240 W/m. K, which is similar to the thermal conductivity value of diamond. However, thermal conductivity value of diamond drops at a faster rate with temperature as compared to BA. At around 400 K, the thermal conductivity value of BA is around 1800 W/m.K as compared to 1500 W/m.K for diamond. Boron arsenide is a face-centered cubic crystal with a lattice constant of 0.4777 nm and an indirect bandgap of roughly 1.46 eV. The structure of boron arsenide is like crystal structure of cubic diamond. The molar mass of boron arsenide is 85.733 g/mol; the large As to B mass ratio causes the atomic motion of the short wavelength acoustic phonons, which give the largest contributions to thermal conductivity, to be dominated by the heavier as mass, and as happens to be isotopically pure.

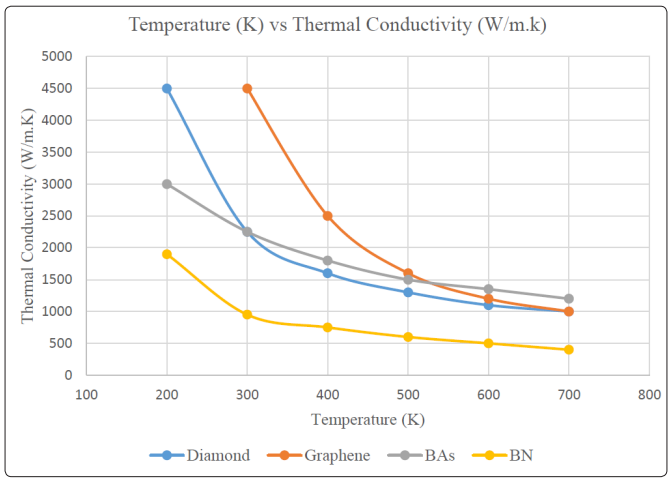

Figure 2: Variation of Thermal Conductivity with Temperature

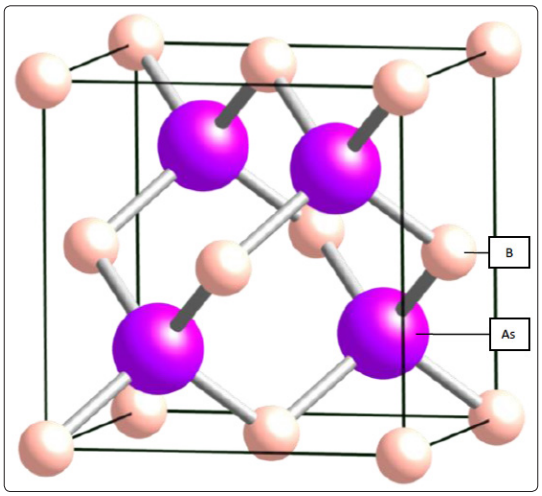

Figure 3: Structure of Boron Arsenide (BAs)

Figure 4 shows the structure of boron arsenide with a rhombohedral structure based on clusters of boron atoms and two-atom As-As chains.

Preparation of Boron Arsenide

Method 1: Elemental boron powder is easily pressed into various shapes by methods of powder metallurgy. Boron particles so produced are exposed to temperatures of about 800 C to 900 C to the vapor of arsenic for the desired length of time. The reaction commences at the surface of the article forming the compound BAs there on and as the treatment is continued the arsenic penetrates the surface and gradually works its way into the center of the particle, converting the entire mass to boron arsenide. The time required for complete reaction is dependent upon the temperature, the mass of material treated, the degree of porosity of the article, the particle size and upon the pressure of arsenic vapor [15].

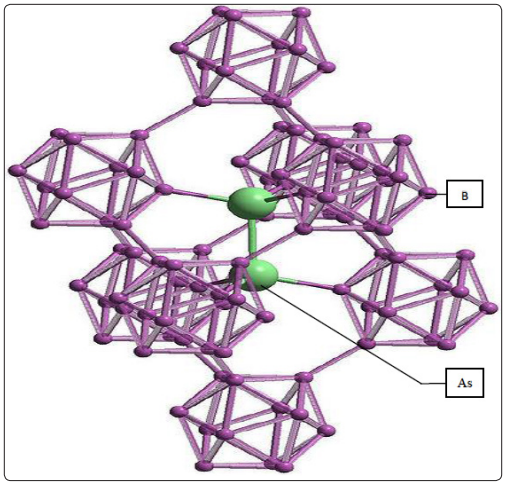

Figure 4: Structure of Boron Arsenide (B12A2)

Method 2: It has been found convenient to carry out this method by charging the desired quantity of solid arsenic into a tubular furnace, heating the said arsenic to vaporize the same while at the same time introducing a gaseous stream of boron trichloride and hydrogen. The product thus obtained is the desired boron arsenide which is removed from the reaction zone and collected in a condenser or other form of relatively cool surface remote from the reaction zone. The product obtained when operating at a temperature of from 700 C to 900 C is the cubic form of boron arsenide, BAs, which is obtained as a black, finely divided powder [15].

Polymer Matrix

Polymeric materials used for the nanocomposite formulation are commercially available "AOS Non-Silicone XT-3" thermal grease and the "EP21TCHT-1" epoxy-based resins. In this work, boron arsenide nanoparticles are considered as the primary candidate to be incorporated in the selected polymer matrix and thermal conductivity is evaluated to ensure the improvement of the thermal properties. Table 1 shows the percentage of filler fraction considered to calculate the value of thermal conductivity for BAs-thermal grease and BAs-epoxy composite thermal interface materials.

Table 1: Percentage of Filler Fraction- Case 1 and Case 2

Percentage of BA Filler (%)	Case 1: "AOS Non- Silicone XT-3" Thermal Grease	Case 2: "EP21TCHT-1" Epoxy
10		
20		
25		
30		
40		
50		

Modeling Thermal Interface Materials

If a heat sink is placed directly on top of a heat-generating device, a thin layer of air gap existsbetween the two mating surfaces due to the roughness and imperfection of the surfaces (Figure 5). The air gaps are thermal barriers to the heat dissipation path. Thermal interface materials (TIM) are used to reduce the air gaps.TIM should have high thermal conductivity, good capability to fill up the micro gaps, and good thermal stability.

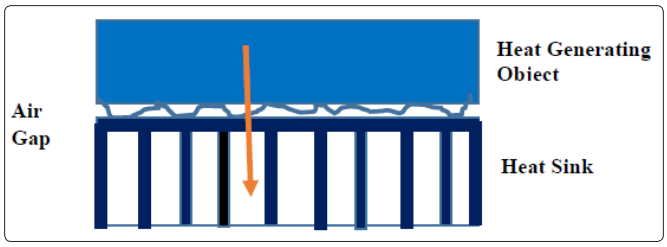

Figure 5: Air Gap vs Thermal Interface Material

The commonly used thermal interface materials are listed in the Table 2.

Table 2: Common Thermal Interface Materials

Type of Material	Thermal Conductivity(W/m.K)	
Gap filler pad	1.5 - 7.0	1.5 - 7.0
Thermal gel	0.7 - 3.5	0.7 - 3.5
Thermal Tapes	0.4 - 1.4	0.4 - 1.4
Thermal grease	0.5 - 3.0	0.5 - 3.0
Epoxy	0.8 - 2.7	0.8-2.7

Parameters Associated with TIM

High thermal conductivity and low thermal resistance of TIM is achieved by dispersing high-conductivity material particles in polymeric base or matrix materials. However, adding these high-conductivity particles also affects the viscosity or fluidity to wet the substrate surfaces and the bond line thickness (BLT) of the TIM as demonstrated in the Figure 6.

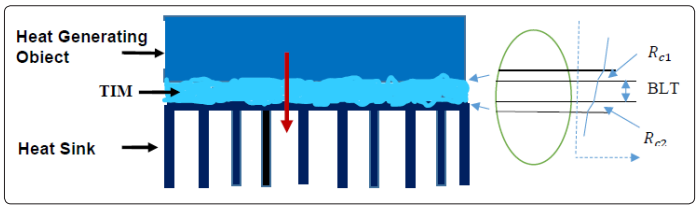

Figure 6: Parameters Associated with Thermal Interface Material

Thermal resistance associated with the bulk TIM is given as

$$R_{TIM,bulk} = \frac{BLT}{K_{TIM}}$$

Thermal resistance of the TIM depends not only on the thermal conductivity but also on the thickness of the BLT. The BLT associated with TIM varies with type and volume fraction of the particles and the applied pressure. The effective thermal conductivity of the TIM has two components: one associated with the bulk resistance of the TIM and second associated with the contact resistances of the TIM with the two substrate interfaces, Rc1 and Rc2 at the top and the bottom respectively. The effective thermal resistance of the TIM is then given as

$$R_{TIM} = R_{TIM,bulk} + R_{c1} + R_{c2}$$

In order to evaluate the effect of type and volume fraction of the high-conductivity nanomaterials on the thermal resistance of the polymer-filler TIM, one also needs to understand its effect on the rheology of the polymer mixture.

In this study, attention is primarily given to the estimation of the thermal conductivity of filler matrix system based on available semi-empirical formulae developed based on effective medium theory (EMT). A separate study is being conducted at NIU about modeling the BLT.

Effective Medium Theory (EMT)

Effective medium theories are the empirical, analytical and numerical models used for predicting the effective thermal conductivity of composite materials using the volume fraction and properties of the filler and matrix material.

Maxwell, Bruggeman, and percolation modelsare the effective medium theories used to create the BAs-thermalgrease and BAs-LO epoxy composite materials. Bond line thickness, particle size, filler fraction, and interfacial thermal resistance coefficient are the properties associated with the effective medium theories used to create the composite materials.

Maxwell Model

Maxwell model is the first analytic expression used to create the composite materials where spherical filler particle with thermal conductivity (Km) are embedded in a continuous matrix of thermal conductivity (Kl).

$$\frac{K_{eff}}{K_m} = 1 + \frac{3 * \emptyset}{\left(\frac{K_l + 2 * K_m}{K_l - K_m}\right) - \emptyset}$$

∅ - Volume fraction of filler
K_{eff} –Effective thermal conductivity of composite material
K_m –Thermal conductivity of matrix material
K_l –Thermal conductivity of filler particle

The drawback of Maxwell model is the value of effective thermal conductivity is valid only for filler fraction up to 25%.

Bruggeman Model

Bruggeman model isaccurate for high filler volume fractions when compared with Maxwell model. The main approaches of this theory assume that a composite material can be incremented by introducing infinitesimal changes to an already existing material.

$$(1 - \emptyset)^3 = \left(\frac{K_m}{K_{eff}}\right)^{\left(\frac{1+2*\alpha}{1-\alpha}\right)} * \left(\frac{(K_{eff} - K_l(1-\alpha))}{(K_m - K_l(1-\alpha))}\right)^{3/(1-\propto)}$$

∅- Volume fraction of filler
K_{eff} –Effective thermal conductivity of composite material
K_m –Thermal conductivity of matrix material
Kl –Thermal conductivity of filler particle
α – (a_k/a)
a – Particle radius
a_k –Kapitza radius= R_b*K_m
R_{int} – Interfacial thermal resistance

The formula to calculate the interfacial thermal resistance is

$$R_b = \frac{(\alpha * a)}{K_m}$$

The interfacial thermal resistance is very low when the particle radius (k_a) is much lesser than the Kapitza radius (a_k); if α = 1; that is, the actual particle radius is equal to a_k then the effective thermal conductivity of the particles is equal to that of the matrix.

If α > 1, that is the particle radius is very small, then the contribution of the particles to the thermal conductivity of the composite is dominated by interfaces; if α < I then the bulk property of the particles is important.

For an efficient thermal conductivity of the composite material the value of 'α' should be in the range of 0.05 to 0.15. The volume filler fraction is directly proportional to the 'α' value; the variation of 'α' value with respect to filler fraction is shown in the Table 3.

Table 3: Variation of 'α' with Volume Filler Fraction of BAs

Volume Filler Fraction	α
< 50 %	0.05
> 50 %	0.15-1.00

Percolation Model

Percolation model is the most effective in determining the effective thermal conductivity of composite materials; theoretical results obtained with the percolation model agree better with the experimental data.

$$\lambda = \lambda_2 * \left(\frac{\lambda_c}{\lambda_2}\right)^{\left[\frac{1-V}{1-V_c}\right]^n}$$

λ – Effective thermal conductivity of percolation model
λ_2– Thermal conductivity of filler particle
λc – Effective thermal conductivity of Bruggeman model
n –Percolation exponent
V – Volume filler fraction
V_c – Percolation threshold

V_c varies from 0.15 to 0.30 and n is expected to be in the range of 0 to 1. Either Maxwell model or Bruggeman model is used to estimate the value of effective thermal conductivity (λ_c); the 'λ_c'value thus obtained is substituted in the percolated model along with the values of V_c, V, λ_2 and n to calculate the effective thermal conductivity of the composite material.

If $\left(\frac{\lambda-\lambda_c}{\lambda_c}\right) \leq 5$ is satisfied, then the assumed value of Vc is accepted. Otherwise, a new value of Vc should be selected and the above procedures are repeated.

The effective thermal conductivity 'λ' reduces to that of the polymer matrix when the volume fraction of filler is zero (V=0). As a result, n is determined by substituting the above estimated values of V_c and λ_c into the percolation model.

Comparison of Effective Medium Theories

Thermal conductivity of filler particle, matrix material, filler fraction, particle radius, thickness, and interference resistance are the variables associated with the three models. Each model includes two or more variables out of all the above-mentioned variables to create the composite thermal interface materials.

Table 4 compares the models in terms of variables associated with each model.

Table 4: Comparison of Effective Medium Theories

Model	K_{matrix}	K_{filler}	∅	R_b	V_c	a
Maxwell	×	×	×			
Bruggeman	×	×	×	×		×
Percolation		×	×		×	

Each model has its own constraint in evaluating the effective thermal conductivity of the composite material. The constraints associated with each model are shown in the Table 5.

Table 5: Constraints Associated with Effective Medium Theories

Model	Constraint	Value
Maxwell	∅	< 25%
Bruggeman	α	< 0.15
Percolation	V_c	0.15 – 0.30

By comparing the end value of all the three models, it is possible to design the BAs-based composite thermal interface materials with optimal thickness, particle radius, interference resistance and minimum filler fraction.

Selection of Matrix Materials

An efficient matrix material should be thermally conductive, electrically insulating, and heat resistant. Based on their properties, non-silicone thermal grease and low outgassing (LO) epoxy are selected as matrix materials to create the BAs based composite thermal interface materials.

Non-silicone Thermal Grease

Non-silicone thermal greases are much efficient than the silicone thermal greases for heat transfer applications. In silicone thermal greases, several thermal cycles cause dry out, interface film cracking, resulting in a loss of thermal conduction; Non-Silicone compounds shows 50% to 80% less oil separations compared to silicone compounds.

For this research, I have used the "AOS Non-Silicone XT-3" thermal grease as one of the matrix materials. Non-Silicone XT-3 is especially appropriate when outgassing is a concern and there is an intentional heat source that requires continuous operation at temperatures exceeding 473K.

The properties of "AOS Non-Silicone XT-3" thermal grease are listed in the Table 6.

Table 6: Properties of "AOS Non-Silicone XT-3" Thermal Grease

Brand	AOS Thermal Compounds
Product	Non-Silicone XT-3
Density	2400 kg/m³
Thermal Conductivity	0.7 W/(m-K)
Specific heat	1000 J/(Kg-K)
Coefficient of thermal expansion	150 µm/(m-°C)

Low Outgassing Epoxy

Epoxy is the most commonly used matrix material to create the composite materials. "Master Bond Polymer System EP21TCHT-1" is the other matrix material used in this research. It is a two-component, thermally conductive, heat-resistant epoxy compound formulated to cure at ambient temperatures or more rapidly at elevated temperatures.EP21TCHT-1 passes NASA outgassing tests and has service temperature range up to 450 K.The properties of "EP21TCHT-1" epoxy are listed in Table 7.

Adding the high thermally conductive filler particles to these matrix material results in the formation of epoxy composites with high thermal conductivity when compared to the start of art thermal interface materials.

Table 7: Properties of "EP21TCHT-1" Epoxy

Brand	Master Bond
Product	EP21TCHT-1
Density	1250 kg/m³
Thermal conductivity	1.44 W/(m-K)
Specific heat	1188 J/(Kg-K)
Coefficient of thermal expansion	20 µm/(m-°C)

Properties of Boron Arsenide

The properties of "Boron Arsenide" are listed in the Table 8.

Table 8: Properties of Boron Arsenide

Density	5220 kg/m³
Thermal conductivity	2200W/(m-K)
Specific heat	417 J/(Kg-K)

The boron arsenide nanoparticles are loaded as filler in the matrix material with filler fraction ranging between 10 % - 95 %.

Calculation of Effective Thermal Conductivity

Maxwell Model

The effective thermal conductivity of the composite material is calculated by varying the boron arsenide (K = 2200 W/m.K) filler fraction from 5 % to 95 %.

Case 1:"AOS Non-Silicone XT-3" Thermal Grease

Thermal conductivity of boron arsenide (filler material) = 2200 W/(m-K).

Thermal conductivity of thermal grease (matrix material) = 0.7 W/(m-K).

Figure 7 shows the variation in effective thermal conductivity of the composite material when the filler fraction is increased in a progressive manner.

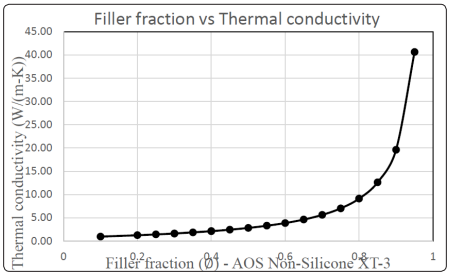

Figure 7: Variation of Thermal Conductivity with BAs Filler Fraction (AOS Non-Silicone XT-3)

The value at 10% filler fraction is 0.93 W/(m-K).
The value at 20% filler fraction is 1.23 W/(m-K).
The value at 25% filler fraction is 1.40 W/(m-K).

Case 2: "EP21TCHT-1" Epoxy

Thermal conductivity of boron arsenide (filler material) = 2200 W/(m-K).
Thermal conductivity of epoxy (matrix material) = 1.44 W/(m-K).

Figure 8 shows the variation in effective thermal conductivity of the composite material when the filler fraction is increased in a progressive manner.

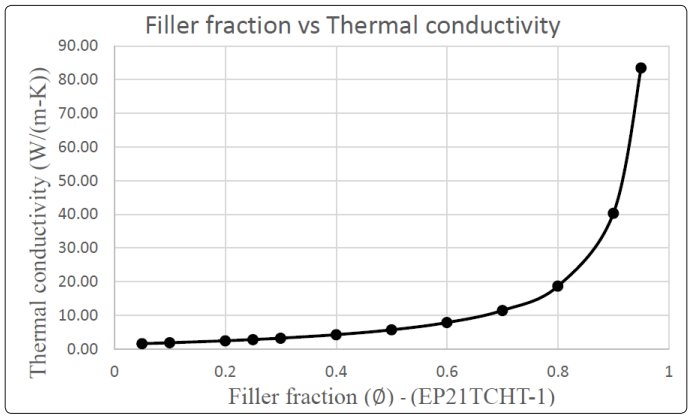

Figure 8: Variation of Thermal Conductivity with BAs Filler Fraction (EP21TCHT-1)

The value at 10% filler fraction is 1.92 W/(m-K).
The value at 20% filler fraction is 2.52 W/(m-K).
The value at 25% filler fraction is 2.88 W/(m-K).

The Maxwell model matches with the experimental data for filler fraction up to 25%. It can be seen from case 1 and case 2, Maxwell model doesn't work well for filler fraction greater than 25%.The thermal conductivity of the composite materials has increased twice the thermal conductivity of the matrix material in both the cases at the filler fraction of 25%.

In Maxwell model, the thermal conductivity of the composite material is not found to increase steadily with increase in the percentage of filler fraction. When the filler fraction is increased above 80%, the thermal conductivity of the composite material rises suddenly which is not valid experimentally?

Bruggeman Model

The effective thermal conductivity of the composite material is calculated by varying the filler fraction from 5 % to 95 %. The 'α' value is taken as 0.06 for filler fraction up to 50% and 0.15 for filler fraction up to 95%.

Case 1: "AOS Non-Silicone XT-3" Thermal Grease"

Thermal conductivity of boron arsenide (filler material) = 2200 W/(m-K).
Thermal conductivity of thermal grease (matrix material) = 0.7 W/(m-K).

Figure 9 shows the variation in effective thermal conductivity of the composite material when the filler fraction is increased in a progressive manner.

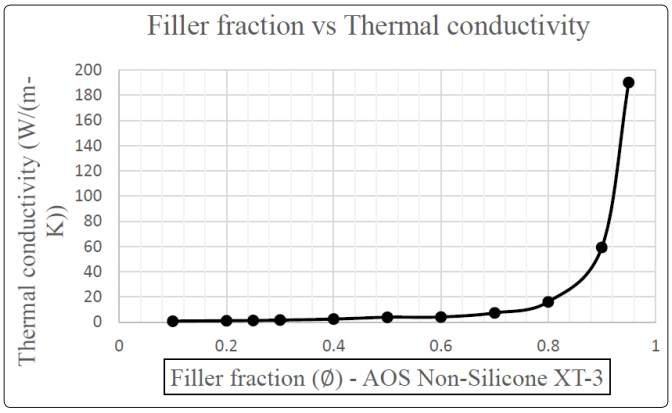

Figure 9: Variation of Thermal Conductivity with BAs Filler Fraction (AOS Non-Silicone XT-3)

Case 2: "EP21TCHT-1" Epoxy

Thermal conductivity of boron arsenide (filler material) = 2200 W/(m-K).
Thermal conductivity of epoxy (matrix material) = 1.44 W/(m-K).

Figure 10 shows the variation in effective thermal conductivity of the composite material when the filler fraction is increased in a progressive manner.

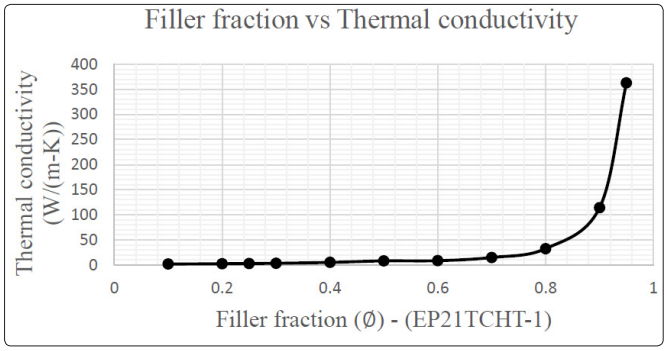

Figure 10: Variation of Thermal Conductivity with BAs Filler Fraction (EP21TCHT-1)

It can be seen from case 1 and case 2, for α = 0.06, the thermal conductivity of Bruggeman model matches closely with the Maxwell model up to filler fraction of 40% and found to be higher than the Maxwell model.

When the filler fraction is increased above 40%, the thermal conductivity of the Bruggeman model is largewhen compared with the Maxwell model.In Bruggeman model, thethermal conductivity of the composite material is found to increase steadily than the thermal conductivity of Maxwell model with the increase in the percentage of filler fraction.

A Comparison of two different TIM based on Bruggeman Model is shown below

Case -1

The value at 30% filler fraction is 1.72 W/(m-K).
The value at 40% filler fraction is 2.52 W/(m-K).
The value at 50% filler fraction is 4.00 W/(m-K).

Case - 2

The value at 30% filler fraction is 3.50 W/(m-K).
The value at 40% filler fraction is 5.20 W/(m-K).
The value at 50% filler fraction is 8.20 W/(m-K).

Percolation Model

Inpercolation model, the effective thermal conductivity of Bruggeman model is used as one of the parametersto calculate the effectivity thermal conductivity.The percolation threshold (Vc) is taken as 0.30 for calculating the effective thermal conductivity.

Case 1: "AOS Non-Silicone XT-3" Thermal Grease

Thermal conductivity of boron arsenide (filler material) = 2200 W/(m-K).
Thermal conductivity of thermal grease (matrix material) = 0.7 W/(m-K).

Figure 11 shows the variation in effective thermal conductivity of the composite material when the filler fraction is increased in a progressive manner.

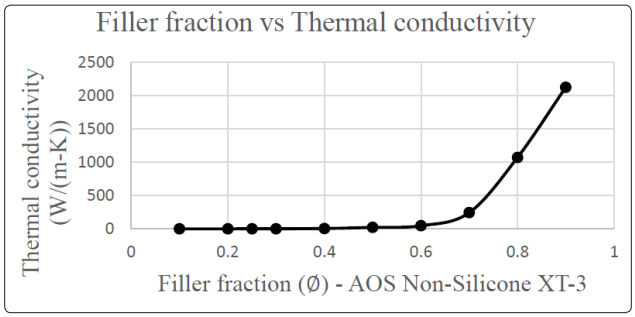

Figure 11: Variation of Thermal Conductivity with BAs Filler Fraction
(AOS Non-Silicone XT-3)

The value at 30% filler fraction is 2.34 W/(m-K).
The value at 40% filler fraction is 6.09 W/(m-K).
The value at 50% filler fraction is 22.66 W/(m-K).

Case 2: "EP21TCHT-1" Epoxy

Thermal conductivity of boron arsenide (filler material) = 2200 W/(m-K).
Thermal conductivity of epoxy (matrix material) = 1.44 W/(m-K).

Figure 12 shows the variation in effective thermal conductivity of the composite material when the filler fraction is increased in a progressive manner.

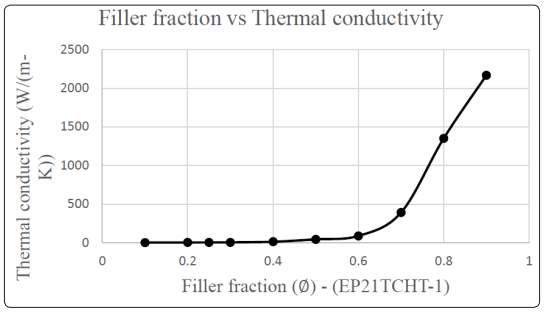

Figure 12: Variation of Thermal Conductivity with BAs Filler Fraction (EP21TCHT-1)

The value at 30% filler fraction is 4.74 W/(m-K).
The value at 40% filler fraction is 12.41 W/(m-K).
The value at 50% filler fraction is 43.93 W/(m-K).

From case 1 and case 2, the thermal conductivity of percolation model matches closely with the Maxwell and Bruggeman model up to filler fraction of 30%. When the filler fraction is increase above 50 %, the thermal conductivity of percolation model is found to be much higher than the thermal conductivity of the Maxwell model and Bruggeman model.

Threshold exponent (n) is the reason for the increase in the thermal conductivity of percolation model. The threshold exponent of less than 1 and $((\lambda-\lambda_c)/\lambda_c) \leq 5$ is satisfied only for filler fraction up to 50%. Therefore, the percolation model has much probability of matching with the experimental results for the filler fraction less than 50%.

Figure 13 shows the variation of threshold exponent for both the case 1 and case 2 with increase in filler fraction from 0 to 90%.

Evaluation of Effective Medium Theories

In all the effective medium theories, the value of thermal conductivity for composite materials is valid for filler fraction only up to 40%.

In Maxwell model, the increase in the thermal conductivity is uncertain and very low for filler fraction greater than 25 %.

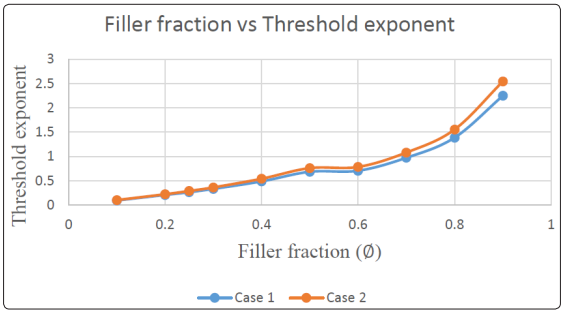

Figure 13: Variation of Threshold Exponent with BAs Filler Fraction

In Bruggeman model, the value of thermal conductivity is very low with the increase in filler fraction up to 75 %. In percolation model, the threshold exponent is within the range for filler fraction less than 50%.The variation in the value of thermal conductivity with increase in filler fraction from 10 to95 % and 10 to 50 % is shown in Figures 14-17 for case 1 and case 2.

Case 1: "AOS Non-Silicone XT-3" Thermal Grease

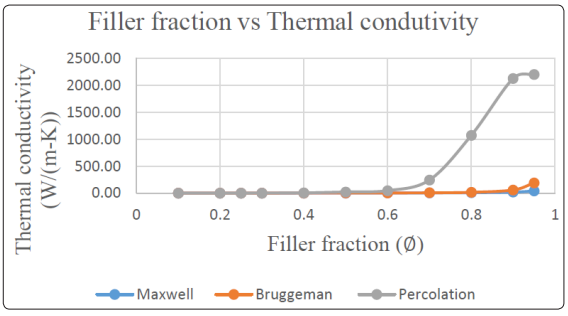

Figure 14: Variation of Thermal Conductivity with BAs Filler Fraction- Case 1 (10 – 95) %

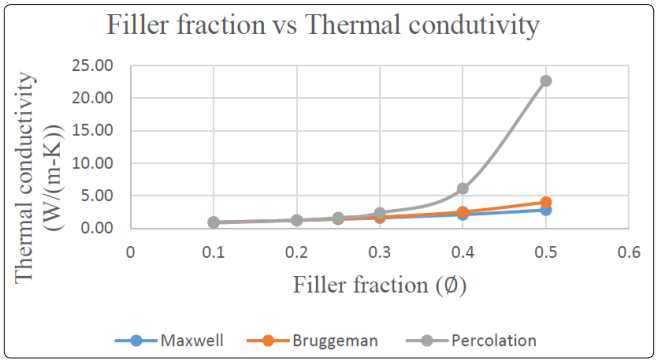

Figure 15: Variation of Thermal Conductivity with BAs Filler Fraction- Case 1 (10 – 50) %

Case 2: "EP21TCHT-1" Epoxy

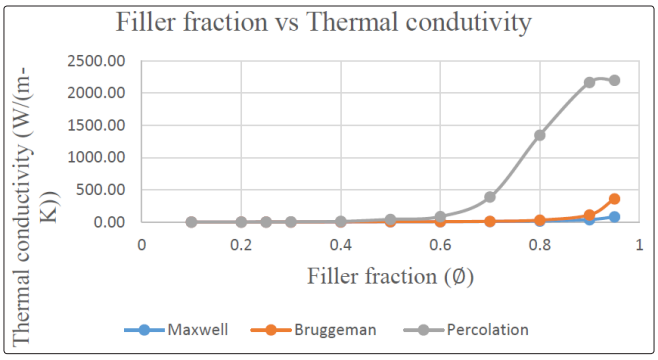

Figure 16: Variation of Thermal Conductivity with BAs Filler Fraction- Case 2 (10 – 95) %

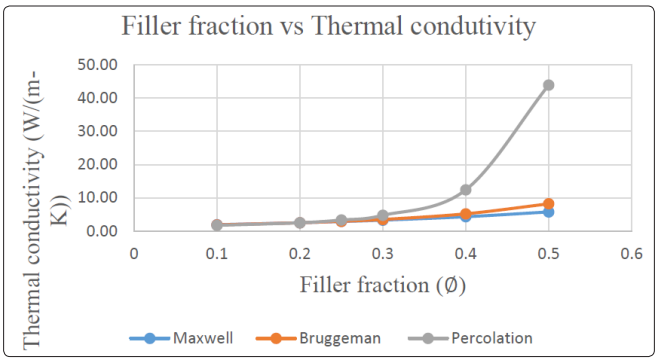

Figure 17: Variation of Thermal Conductivity with BAs Filler Fraction- Case 2 (10 – 50)

References

1. L Lindsay, D Broido and T Reinecke (2013) "First-Principles Determination of Ultrahigh Thermal Conductivity of Boron Arsenide: A Competitor for Diamond?" APS Journals 111: 5.
2. RS Prasher, J Shipley, S Prstic, Koning Paul, J-L Wang (2003) "Thermal Resistance of Particle Laden Polymeric Thermal inferace Materials," Journal of Heat Transfer 125: 8.
3. AL Moore, L Shi (2014) "Emerging Challenges and Materials for Thermal Management of Electronics," Materials Today 17: 12.
4. A Jain, AJ McGaughey (2014) "Thermal Conductivity of Compound Semiconductors: Interplay of Mass Density and Acoustic-Optical Phonon Frequency Gap," Journal of Applied Physics 117: 7.
5. K Pietrak, TS Wisniewski (2015) "A Review of Models for Effective Thermal Conductivity of Composite Materials," Journal of Power Technologies 25: 11.
6. X-Q Wang, AS Mujumdar (2008) "A REVIEW ON NANOFLUIDS - PART I: THEORETICAL AND NUMERICAL," Brazilian Journal 25: 613-630.
7. F Kargara, AA Balandin, J Renteriab, S Legedzab, R Salgadoa (2014) "A comparative study of the thermal interface materials with graphene and boron nitride fillers," in The International Society for Optical Engineering , Riverside.
8. F Sarvar, DC Whalley, PP Conway (2006) "Thermal Interface Materials - A Review of the State of the Art," in Electronic System Integration Technology Conference, Dresden.
9. Y Tao, S Tu, G Zhang, Y Xia, W Hui, et al. (2010) "A Percolation Model of Thermal Conductivity for Filled Polymer Composites," Journal of Composite Materials 44: 963-969.
10. RR Syamala (2016) "Computational Analysis of IGBT Package Using Graphene Composites as Thermal Interface Materials," Northern Illinois University, DeKalb.
11. E Pop, V Varshney, AK Roy (2012) "Thermal properties of graphene: Fundamentals and applications," MRS Bulletin 37: 1273-1281.
12. AA Balandin, DL Nika (2015) "Thermal Transport in Graphene and Graphene Multilayers," University of California, Moldova State University, Riverside, Chisinau.
13. D Signh, JY Murthy, TS Fisher (2011) "Mechanism of thermal conductivity reduction in few-layer graphene," Birck and NCN Publications, West Lafayette.
14. N Hosmane (2011) "http://www.niutoday.info," Northern Illinois University. Available: http://www.niutoday.info/2011/06/20/team-of-niu-scientists-discovers-simple-green-method-of-producing-highly-touted-graphene/.
15. WV Forrest (1968) "Process for preparing crystalline boron arsenide". Dayton/ Ohio Patent US 3413092 A.
16. A Chakrabarti, P Majumdar (2017) "Graphene and boron nitride-based nanocomposites with enhanced thermal properties," Northern Illinois University, Applied Material Systems Engineering Inc., DeKalb.